Dissociative Recombination of Protonated Formic Acid: Implications for Molecular Cloud and Cometary Chemistry

Vigren, E., Hamberg, M., Zhaunerchyk, V., Kaminska, M., Semaniak, J., LArsson, M., ... Geppert, W. D. (2010). Dissociative Recombination of Protonated Formic Acid: Implications for Molecular Cloud and Cometary Chemistry. Astrophysical Journal, 709, 1029-1034. DOI: 10.1088/0004-637X/709/2/1429

Published in:
Astrophysical Journal

The Astrophysical Journal, 709:1429–1434, 2010 February 1 doi:10.1088/0004-637X/709/2/1429

DISSOCIATIVE RECOMBINATION OF PROTONATED FORMIC ACID: IMPLICATIONS FOR MOLECULAR CLOUD AND COMETARY CHEMISTRY

E. Vigren[1,2,6], M. Hamberg[1], V. Zhaunerchyk[1,3], M. Kaminska[4], J. Semaniak[4], M. Larsson[1], R. D. Thomas[1], M. af Ugglas[1], I. Kashperka[1], T. J. Millar[5], C. Walsh[5], H. Roberts[5], and W. D. Geppert[1,7]
[1] Department of Physics, AlbaNova, Stockholm University, SE-10691 Stockholm, Sweden; wgeppert@hotmail.com
[2] Astrobiology Graduate School, Stockholm University, Stockholm, Sweden
[3] Institute for Molecules and Materials, Radboud University Nijmegen, P.O. Box 9010, NL-6500 GL Nijmegen, The Netherlands
[4] Institute of Physics, Jan Kochanowski University, Świętokrzyska 15, PL-25406 Kielce, Poland
[5] Astrophysics Research Centre, School of Mathematics, and Physics, Queen's University Belfast, Belfast BT7 1NN, UK
Received 2009 October 21; accepted 2009 December 18; published 2010 January 13

ABSTRACT

At the heavy ion storage ring CRYRING in Stockholm, Sweden, we have investigated the dissociative recombination of $DCOOD_2^+$ at low relative kinetic energies, from ∼1 meV to 1 eV. The thermal rate coefficient has been found to follow the expression $k(T) = 8.43 \times 10^{-7}\ (T/300)^{-0.78}$ cm^3 s^{-1} for electron temperatures, T, ranging from ∼10 to ∼1000 K. The branching fractions of the reaction have been studied at ∼2 meV relative kinetic energy. It has been found that ∼87% of the reactions involve breaking a bond between heavy atoms. In only 13% of the reactions do the heavy atoms remain in the same product fragment. This puts limits on the gas-phase production of formic acid, observed in both molecular clouds and cometary comae. Using the experimental results in chemical models of the dark cloud, TMC-1, and using the latest release of the UMIST Database for Astrochemistry improves the agreement with observations for the abundance of formic acid. Our results also strengthen the assumption that formic acid is a component of cometary ices.

Key words: astrochemistry – molecular processes

1. INTRODUCTION

Formic acid (HCOOH), the simplest organic acid, has been observed in a variety of extraterrestrial environments. The first reported detection was toward the Sgr B2 region by Zuckerman et al. (1971) and Winnewisser & Churchwell (1975). Liu et al. (2001) carried out a survey of HCOOH toward eight galactic hot molecular cores and detected the molecule in three of these sources (Sgr B2, Orion KL, and W51). Based on a correlation between HCOOH and methyl formate ($HCOOCH_3$) emission in these three regions, the authors argued that the molecule is produced in processes related to grain-surface chemistry and mantle evaporation. The non-detection of HCOOH toward G34.3 + 0.2 and W3(H_2O) was attributed to a generally lower abundance in these regions such that the column densities of HCOOH were below the detection limit. In two other sources, NGC 7538 IRS1 and NGC 7538 IRS9, the lack of signals was argued to be due to the fact that HCOOH (as well as other complex species) is still frozen out on grain surfaces, which is indicated by the observations of possible IR spectral features of HCOOH in the solid state. Garrod & Herbst (2006) studied the evolution of HCOOH and other organic species in the warm up phase of hot molecular cores by means of a gas–grain chemical network. Their model produced HCOOH and other complex organic species in large abundances during the protostellar switch-on phase, both by grain-surface and gas-phase processes. The authors argued that the most likely route to HCOOH is by the reaction HCO + OH → HCOOH on surfaces.

Irvine et al. (1990) performed a survey of HCOOH in two nearby cold dark clouds, TMC-1 and L134N. It was firmly detected only in L134N, with an abundance of N(HCOOH)/$N(H_2) \sim 3 \times 10^{-10}$. An upper limit of N(HCOOH)/$N(H_2) \sim 2 \times 10^{-10}$ was reported by Ohishi et al. (1992) in the well-studied dark cloud TMC-1. A gas-phase only chemical model of TMC-1, which employs physical parameters and rate coefficients according to the latest version of the UMIST Database for Astrochemistry (Woodall et al. 2007; http://www.udfa.net), overestimates the HCOOH abundance by about an order of magnitude. One of the key reactions for the synthesis of HCOOH in this model is the dissociative recombination (DR) of protonated formic acid, $HCOOH_2^+$ (which has the structure $HC(OH)_2^+$):

$$HCOOH_2^+ + e^- \rightarrow HCOOH + H. \quad (1)$$

During the last few years, experiments have shown that several protonated ions do not tend to just eject a hydrogen atom upon DR: the breaking of bonds between heavy atoms and fragmentation into three or even more products has also been observed. As an example, the DR of protonated methanol was found to produce methanol in only ∼3% of the reactions (Geppert et al. 2006). In the UMIST code only the channel leading to HCOOH + H (i.e., reaction (1)) is included, with an estimated rate coefficient of $3.0 \times 10^{-7}\ (T/300)^{-0.50}$ cm^3 s^{-1} for the DR of protonated formic acid. To test the validity of this assumption and with the aim to improve the astrochemical models, we have investigated the DR of protonated formic acid at the heavy ion storage ring CRYRING at the Manne Siegbahn Laboratory in Stockholm, Sweden. We present in this paper the results (thermal rate coefficient and branching fractions) of this experiment and their implications for the predicted abundance of formic acid in TMC-1 and L134N. Finally, we briefly discuss cometary HCOOH in light of the experimental results.

2. EXPERIMENTAL OVERVIEW

The heavy ion storage ring CRYRING and the typical procedure of DR experiments have been described previously (e.g.,

[6] http://www.astrobiology.physto.se
[7] Corresponding author.

Strömholm et al. 1996; Neau et al. 2000). In this experiment fully deuterated formic acid (DCOOD) and D_2 were mixed in a hollow cathode discharge ion source (Peterson et al. 1998) and, periodically, a ∼kV discharge was introduced in the source, ionizing the source gases, and triggering ion–molecule reactions. Due to experimental reasons (e.g., improved resolution and detection efficiency and a lower risk of contamination) fully deuterated protonated formic acid, $DCOOD_2^+$, was studied in the present experiment. It should be noted that the branching fractions determined for the DR of hydrogen containing molecular ions in several experiments have been shown to be similar to their deuterated analogs (e.g., Neau et al. 2000; Geppert et al. 2006). However, although isotopic effects have been observed in the rate coefficients for smaller ions (e.g., H_3O^+/D_3O^+; Neau et al. 2000), such differences have been shown to be small or negligible in studies of larger ions (e.g., $CH_3OH_2^+/CD_3OD_2^+$; Geppert et al. 2006), CH_2OH^+/CD_2OD^+ (Hamberg et al. 2007). We believe therefore that our results regarding the DR of $DCOOD_2^+$ are indicative of the DR of $HCOOH_2^+$.

The ions were extracted from the source and accelerated by a potential of 40 kV and mass selected by a bending magnet before being injected into the storage ring (circumference 51.6 m). Given the initial gas mixture in the ion source, DCOOD and D_2, ions with $m/z = 50$ injected into the ring should have been protonated formic acid with the precise structure $DC(OD)_2^+$. In support of this Sekigushi et al. (2004) concluded from mass-spectrometric investigation and ab initio calculations that protonation occurs only on the carbonyl oxygen of formic acid. Some contamination by ions produced via reactions amongst DCOOD fragments cannot be completely ruled out. A mass-to-charge spectrum of ions extracted from the source was recorded, which indicated that DCOOD molecules did not fragment to a large extent; the highest current was found for $m/z = 50$ with $m/z = 48$ being the second strongest.

After injection into the ring the ions were further accelerated to 1.9 MeV (the highest possible kinetic energy for singly charged ions of mass 50 amu at CRYRING) by a radio frequency system. Over a length of 0.85 m, in an electron cooler, the ions were merged with a homogeneous electron beam of radius $r_e = 2$ cm and with a current of $I_e = 0.305$ mA. The electrons had a longitudinal and transversal energy spread of ∼0.1 and ∼2 meV, respectively (Danared et al. 2000), and served partly to cool down the ion beam (phase space reduction) but mainly as a reaction target.

The number of reactions between ions and residual gas was monitored versus storage time using a microchannel plate (MCP) detector located in one of the straight sections of the ring. This number was proportional to the ion current. The absolute ion current was measured during the 1.0 s long acceleration phase by a capacitive pick up calibrated to an AC transformer (Paál et al. 2006). At the end of the acceleration phase, the proportionality between the ion current and the number of recorded background signals was established.

Neutral products produced in the interaction region either from DR or from reactions of the ions with the residual gas molecules, unaffected by the bending magnet located after the interaction region, left the ring tangentially and hit an energy sensitive ion implanted silicon detector (IISD). By connecting the IISD via amplifiers and a discriminator to a multichannel scaler (MCS), the number of DR reactions versus storage time was recorded for cross section measurements. Connecting the IISD via amplifiers to a multichannel analyzer (MCA) gave a spectrum displaying counts versus kinetic energy of the fragments impinging the detector (for measuring branching fractions). Prior to the data acquisition, the electrons were tuned to the same average velocity as the ion beam for 3.0 s in order to cool the ion beam. The storage time also allowed ions produced in vibrationally excited states to spontaneously relax by photon emission. Having vibrationally relaxed ions is of importance for the validity of our results as input in astrochemical models, since vibrational excitations are rare under dark cloud conditions.

3. DATA ANALYSIS AND RESULTS

3.1. Cross Section and Thermal Rate Coefficient

For cross section measurements, the cathode voltage of the electron cooler was linearly scanned over a period of 2.0 s. At the beginning of the ramp, the electrons are faster than the ions and the relative kinetic energy (i.e., sum of the kinetic energies of the particles relative to the centre of mass) was ∼1 eV. At the end of the ramp, the relative kinetic energy was again ∼1 eV but now with the ions being faster than the electrons. During this ramp, the count rates from the DR reactions were measured by means of the IISD connected to the MCS card. Subtraction of signals arising from reactions between the ions and the residual gas was done using the fact that the DR cross section is typically very small at relative kinetic energies of 1 eV (Hellberg et al. 2005). Signals recorded at these energies are attributed to non-DR processes and could be fitted to an exponential curve with a decay constant similar to that of the ion beam intensity as recorded by the MCP detector. The DR rate coefficient, α, is derived from known quantities as

$$\alpha = \langle \sigma v_{\rm rel} \rangle = \frac{dN_{\rm DR}}{dt} \frac{q^2 v_e v_{\rm ion} \pi r_e^2}{I_e I_{\rm ion} l}, \quad (2)$$

where $dN_{\rm DR}/dt$ is the DR count rate, q is the elementary charge, v_e and $v_{\rm ion}$ are the electron and ion velocities, respectively, I_e and $I_{\rm ion}$ are the electron and ion currents, respectively, r_e denotes the radius of the electron beam, and l is the length of the interaction region. The DR rate coefficient was corrected for the space charge effect (DeWitt et al. 1996) and for the DR reactions occurring at higher collision energies in the regions of the electron cooler where the electron beam was bent into and out of the ion beam by toroidal magnets (Lampert et al. 1996). The DR cross section versus relative kinetic energy was extracted from the DR rate coefficient (see Mowat et al. 1995) using the expression

$$\langle \sigma v_{\rm rel} \rangle = \int v_{\rm rel} f(v_{\rm rel}) \sigma(v_{\rm rel}) d^3 v_{\rm rel}, \quad (3)$$

where $f(v_{\rm rel})$ is the relative velocity distribution. The cross section versus relative kinetic energy for the DR of $DCOOD_2^+$ is shown in Figure 1.

The data can be fitted by

$$\sigma(E/{\rm eV}) = 5.8 \times 10^{-16} (E/{\rm eV})^{-1.28}\ {\rm cm}^2 \quad (4)$$

for relative kinetic energies of 1 meV $< E <$ 0.1 eV. For relative kinetic energies >0.1 eV, the DR cross section drops as $(E/{\rm eV})^{-1.88}$. Folding the DR cross section with an isotropic Maxwellian distribution of electron speeds yields the thermal rate coefficient:

$$k(T) = \left(\frac{m_e}{2\pi k_B T} \right)^{3/2} \int_0^\infty v \sigma(v) e^{-\frac{m_e v^2}{2k_B T}} 4\pi v^2 dv, \quad (5)$$

Table 1
Exoergic Channels in the Reaction $DCOOD_2^+$ + Electron at 0 eV Relative Kinetic Energy

Channel	Products	Kinetic Energy Released (eV)	Channel	Products	Kinetic Energy Released (eV)
1*a*)	DCOOD + D	5.8	1*m*)	DCO + O + D_2	1.1
1*b*)	DOCO + 2D	1.5	1*n*)	DCO + OD + D	1.0
1*c*)	DCO_2 + 2D	0.9	1*o*)	COD + D_2O	6.9
1*d*)	DOCO + D_2	6.1	1*p*)	COD + O + D_2	1.7
1*e*)	DCO_2 + D_2	5.5	1*q*)	COD + OD + D	1.7
1*f*)	CO_2 + D_2 + D	6.0	1*r*)	CO + D_2O + D	5.6
1*g*)	CO_2 + 3D	1.5	1*s*)	CO + OD + D_2	4.9
1*h*)	CD_2OD + O	1.9	1*t*)	CO + OD + 2D	0.4
1*i*)	D_2CO + OD	4.9	1*u*)	CO + O + D_2 + D	0.5
1*j*)	D_2CO + O + D	0.5	1*v*)	CD_3 + O_2	2.7
1*k*)	DCOD + OD	2.6	1*w*)	CD_2 + O_2D	0.03
1*l*)	DCO + D_2O	6.2			

Note. The kinetic energy released have been calculated using heats of formation compiled from Leach et al. (2006), Matus et al. (2006), the NIST Chemistry Webbook (2005), and Lias et al. (1988).

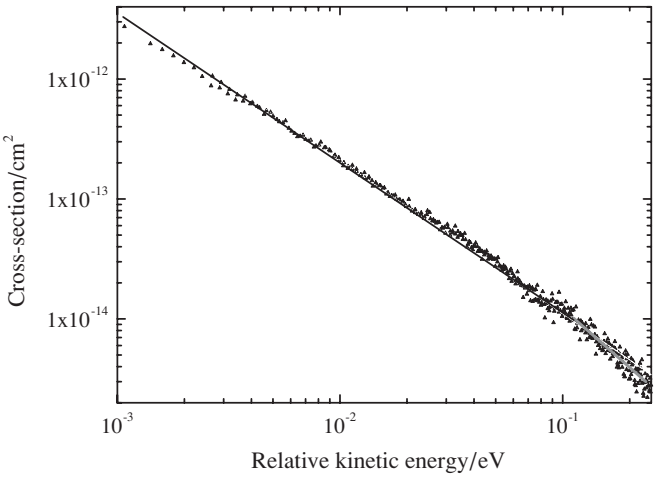

Figure 1. Absolute DR cross section versus relative kinetic energy in the DR of $DCOOD_2^+$. The black line shows the best fit of the data for relative kinetic energies ranging from 1 meV to 0.1 eV (given by Equation (4)). The gray line fits data points above 0.1 eV.

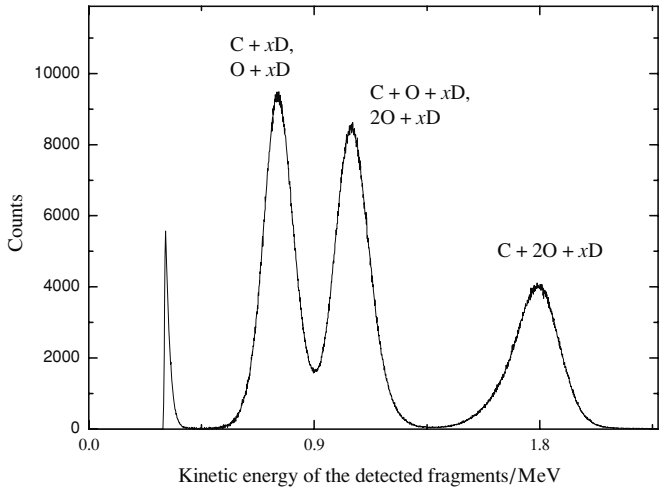

Figure 2. Background-subtracted energy spectra recorded at ~2 meV relative kinetic energy between the electrons and ions (grid inserted) for the DR of $DCOOD_2^+$. The structure to the left is due to noise in mixture with D-atoms. Signals corresponding to energies below ~0.4 MeV were discriminated to reduce the dead time of the measurement system.

where T is the electron temperature and k_B is Boltzmann's constant. The thermal rate coefficient was best fitted by

$$k(T) = 8.43 \times 10^{-7}(T/300)^{-0.78}\ \mathrm{cm}^3\ \mathrm{s}^{-1}. \quad (6)$$

For the DR cross section systematic uncertainties include, e.g., the electron beam radius, the length of the interaction region, and the ion beam circumference. Statistical uncertainties include, e.g., uncertainties in counts from DR events. The estimated uncertainties for the DR cross section below 0.1 eV (where the count rate was high) and the thermal rate coefficient below 1000 K is ~15%–20%.

3.2. Branching Fractions

The integration time of the detector was longer than the difference in the time of flight of fragments originating from the same DR event and hence the detector recorded the total kinetic energy of fragments from a single DR event. The branching fractions were investigated at ~2 meV relative kinetic energy by means of the grid technique (see Neau et al. 2000 for details). In brief a grid with a transmission probability of $P = 0.297 \pm 0.015$ was inserted in front of the detector giving a pulse height spectrum containing a series of peaks instead of only one peak corresponding to the total mass of the DR fragments, which typically is the case when the grid is not inserted. Contributions from non-DR processes were accounted for by recording an MCA spectrum at ~1 eV. Signals recorded during this measurement were essentially only from non-DR processes and as such non-DR contributions could be subtracted from the MCA spectrum recorded at ~2 meV by normalizing the two MCA spectra according to the intensity of the ion beam as recorded by the MCP detector.

In the DR of $DCOOD_2^+$, the channels in Table 1 are exoergic at 0 eV relative kinetic energy.

Figure 2 shows the background-subtracted pulse height spectrum recorded for the DR of $DCOOD_2^+$ and it can be seen that the detector resolution was insufficient to resolve light fragments (D-atoms) and fragments differing only by a few amu in mass. As such we could only gain information about the probabilities of fragmentations of bonds between heavy atoms.

There is no exoergic channel leading to three fragments which each contain one heavy atom. In the channels 1*a*)–1*g*) the heavy atoms remain in the same fragment upon DR while in 1*h*)–1*w*) one bond between heavy atoms is broken. The relative importance of the two different types of fragmentations, 1*a*)–1*g*) versus 1*h*)–1*w*), was determined by solving a system of linear equations. Reactions of the type 1*a*)–1*g*) could only contribute

to the peak labeled C + 2O + xD and did so if the heavy fragment passed the grid which had a probability of P. The channels 1h)–1w) could contribute to all peaks, from left to right in Figure 2, with probabilities of $P(1-P)$, $P(1-P)$, and P^2, respectively. The branching fractions were accordingly obtained by solving the equation system

$$\begin{bmatrix} I_1 + I_2 \\ I_3 \end{bmatrix} = \begin{bmatrix} 0 & 2P(1-P) \\ P & P^2 \end{bmatrix} \times \begin{bmatrix} N_{1a-1g} \\ N_{1h-1w} \end{bmatrix} \quad (7)$$

in which I_1, I_2, and I_3 are the intensities of the peaks labeled "C + xD, O + xD", "C + O + xD, 2O + xD," and "C + 2O + xD" in Figure 2, respectively, and N_{1a-1g}, N_{1h-1w} are the (unknown) numbers of reactions of types 1a)–1g) and 1h)–1w), respectively. Solving the system of Equation (7) and after normalization of the results, the branching fractions in the DR of $DCOOD_2^+$ are found to be

$$\begin{aligned} \phi(1a-1g) &= 0.13 \pm 0.03 \\ \phi(1h-1w) &= 0.87 \pm 0.03. \end{aligned} \quad (8)$$

This implies that in ~13% of the DR reactions the heavy atoms remain in the same product fragment (i.e., channel 1a)–1g)), whereas ~87% of the reactions involve a break of a bond between heavy atoms leading to two heavy fragments, one with two heavy atoms and one with one heavy atom (i.e., channel 1h)–1w)). The quoted uncertainties are mainly due to the uncertainty in the transmission probability of the grid.

The effect of rotational excitation on rate coefficients and branching fractions has been experimentally studied for H_3^+. It has been shown that rotationally cold H_3^+ (T_{rot} ~ 30 K) has a ~40% lower thermal rate coefficient than rotationally hot H_3^+ (T_{rot} possibly a few thousand K) at a kinetic temperature of 300 K (McCall et al. 2004; Sundström et al. 1994). The branching fractions of the H_2 + H and H + H + H channels were also slightly affected by the rotational temperature. For rotationally hot ions, ~75% of the DR reactions lead to H + H + H (Datz et al. 1995), while for rotationally cold ions H + H + H was produced in 64% ± 5% of the DR reactions (McCall et al. 2004). It must be stressed that H_3^+ lacks a permanent dipole moment meaning that its rotational temperature does not change much during typical storage times. Strasser et al. (2002) showed, for example, that the rotational temperature of H_3^+ after 40 s of storage in the Test Storage Ring in Heidelberg still was ~3500 K. Contrary, $DCOOD_2^+$ possesses a permanent dipole moment and we expect therefore that the rotational temperature of the ions was ~300 K during the data acquisition from DR events in the present experiment. We are not completely sure how the DR thermal rate coefficient and branching fractions are affected by the rotational state of the ion, but we think that the results we have presented in this paper are valid to use in models of dark clouds, hot cores, and cometary comae as the difference in rotational energy is only a few tens of meV when comparing T_{rot} = 300 K with, for example, a typical dark cloud T_{rot} of ~10–20 K.

4. DISCUSSION

4.1. Astrochemical Implications

4.1.1. Formic Acid in the Dark Cloud TMC-1

The cold dark cloud TMC-1 is a well-studied object (see, e.g., Pratap et al. 1997; Smith et al. 2004) with well-established physical parameters and chemical abundances and therefore it is a suitable source with which to compare results from astrochemical models. Running a single point pseudo-time-dependent gas-phase chemical model of a dark cloud using the dipole-enhanced version of the latest release of the UMIST Database for Astrochemistry (Woodall et al. 2007; http://www.udfa.net, henceforth referred to as Rate06) with physical parameters appropriate for TMC-1 (T = 10 K, $n(H_2) = 10^4$ cm^{-3}, A_v = 15 mag) and initial elemental abundances as listed in Table 8 of Woodall et al. 2007, gives N(HCOOH)/$N(H_2)$ = 1.1 and 2.1 × 10^{-9} for cloud ages of 1 and 2 × 10^5 yr, respectively. Accordingly, as mentioned in Section 1, our model over predicts the abundance of HCOOH by about an order of magnitude compared with the upper limit of 2 × 10^{-10} with respect to the abundance of H_2 (Ohishi et al. 1992). In this model, formic acid is mainly formed by reaction (1), i.e., by the DR of $HCOOH_2^+$, which in turn is produced mostly via the radiative association reaction

$$HCO^+ + H_2O \rightarrow HCOOH_2^+ + h\nu \quad (9)$$

and the ion-neutral reaction

$$O_2^+ + CH_4 \rightarrow HCOOH_2^+ + H. \quad (10)$$

Up to a time, t ~ 10^4 yr, reaction (9) almost completely dominates the production of $HCOOH_2^+$ whereas the importance of reaction (10) becomes significant only when the chemistry of the cloud is more evolved (at t ~ 10^5 yr). The rate coefficient used for reaction (9) has been determined theoretically (Herbst 1985) and for Equation (10) experimentally (Rowe et al. 1984). As for the ion-neutral reaction $CH_4 + O_2^+$ Van Doren et al. (1986) reported that the structure of the product ion is CH_2OOH^+ (i.e., with the oxygen atoms bonded to each other) and not protonated formic acid. DR of such an ion would require extensive rearrangement of the constituent atoms in order to yield formic acid. We removed reaction (10) from our reaction set to investigate the consequences and found that it only had a very small effect (a decrease of a few percent) on the calculated abundance of HCOOH at t = 1 and 2 × 10^5 yr.

We then instead modified Rate06 to include our experimental findings. In accordance with Equations (6) and (8), we set the rate coefficient for reaction (1) to 1.1 × 10^{-7} $(T/300)^{-0.78}$ cm^3 s^{-1}. This represents an upper limit of the thermal rate coefficient for reaction (1) as determined by our experiment. We also added a channel representative of the reactions 1h)–1w),

$$HCOOH_2^+ + e^- \rightarrow HCO + OH + H \quad (11)$$

with a rate coefficient of 7.3 × 10^{-7} $(T/300)^{-0.78}$ cm^3 s^{-1}. We were mainly interested in comparing the abundance of HCOOH in TMC-1 predicted by the model with the observed upper limit. We could have used any or several of 1h)–1w) (replacing the D-atoms by H atoms) instead of Equation (11) without affecting the overall chemistry in a notable sense, the objective was to introduce a competing channel to reaction (1). Running this model gives N(HCOOH)/$N(H_2)$ = 1.2 and 2.0 × 10^{-10} for cloud ages of 1 and 2 × 10^5 yr, respectively, which is consistent with the upper limits inferred from observations. Figure 3 shows the evolution of the HCOOH abundance in TMC-1 as predicted by our model with and without modification for our results regarding the DR of protonated formic acid.

4.1.2. Formic Acid in the Dark Cloud L134N

We have also run models of the dark cloud L134N (also known as L183). The gas-phase reaction set used for L134N was the

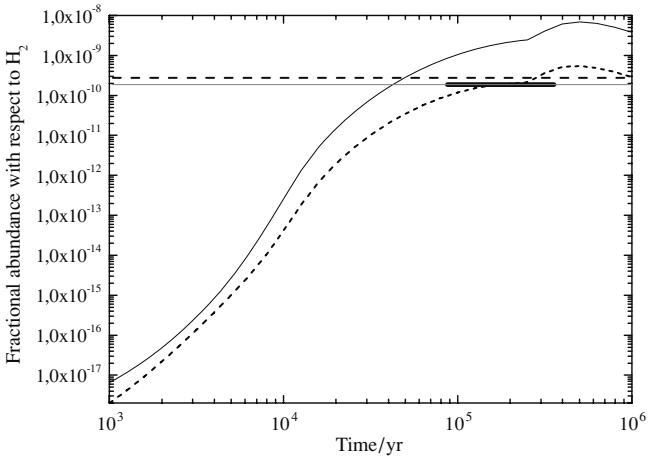

Figure 3. Evolution of HCOOH in TMC-1 using the latest release of the UMIST Database for Astrochemistry (solid black curve). The dotted line is the result from the model including the branching fractions and thermal rate coefficient for the dissociative recombination of protonated formic acid as determined by our experiment. The gray horizontal line represents the upper limit for the abundance of HCOOH in TMC-1 as given in Ohishi et al. (1992). The bold black part of this line is located roundabout the estimated chemical age of TMC-1 ($\sim 10^5$ yr). The dotted horizontal line is the abundance of HCOOH in L134N as given by Irvine et al. (1990).

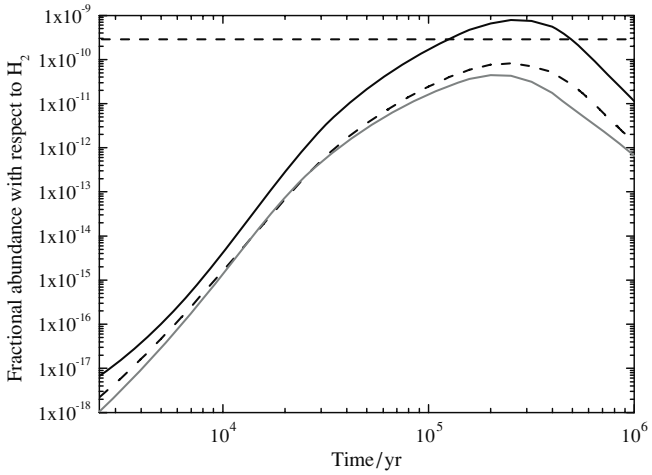

Figure 4. Evolution of HCOOH in L134N using the latest release of the UMIST Database for Astrochemistry (solid black curve) with a C/O ratio of 0.4. The dashed curve and the gray curve are the results of the model including the branching fractions and thermal rate coefficient for the dissociative recombination of protonated formic acid as determined in this paper, with C/O ratios of 0.4 (dashed) and 0.7 (gray). All three models were run allowing the density to increase with time and including the depletion of gas-phase molecules onto dust grains. The dashed horizontal line is the abundance of HCOOH in L134N as given by Irvine et al. (1990).

same as for our model of TMC-1: i.e., the dipole-enhanced version of Rate06 with initial elemental abundances as listed in Woodall et al. (2007). We also assume a cloud temperature of 10 K. L134N was long thought to be a quiescent dark cloud, very similar to TMC-1 (e.g., Terzieva & Herbst 1998; Dickens et al. 2000). Observations of enhanced deuterium fractionation (Roueff et al. 2000; Crapsi et al. 2005) and embedded high-density clumps (Ward-Thompson et al. 1999; Pagani et al. 2003, 2005), however, indicate the presence of "prestellar cores," where molecules are freezing onto the surface of dust grains, indicating L134N is a more evolved object than TMC-1. We have, therefore, run a chemical model of L134N in which we allow the density to increase with time and which also includes the depletion of gas-phase molecules onto dust grains (see, e.g., Roberts & Millar 2000) in order to compare our calculated abundance of HCOOH with that observed toward L134N (Irvine et al. 1990). The freezeout of HCOOH follows CO, which is seen to be heavily depleted in the highest density regions of L134N and so the observed HCOOH is likely to be located in the less dense regions of the cloud where physical conditions are similar to those found in dark clouds. We have also investigated varying the elemental C/O ratio, since Terzieva & Herbst (1998) and Roberts & Herbst (2002) found some evidence for better overall agreement between models and observations with a higher C/O ratio. In Figure 4, we show the observed abundance of HCOOH in L134N alongside model predictions of its evolution. Assuming a chemical age of 2×10^5 yr (see, e.g., Dickens et al. 2000), the calculated abundance of HCOOH goes from being a factor of $\sim$2 higher, to a factor of $\sim$4 lower (C/O ratio of 0.4 in both cases) than the observed value when including the results from our DR investigation.

4.1.3. Formic Acid in the Coma of Comet Hale–Bopp

Bockelée-Morvan et al. (2000) reported the first detection of HCOOH in a cometary coma (Hale–Bopp) and calculated its abundance relative to H_2O ($\sim$0.09%). Rodgers & Charnley (2001) showed that gas-phase chemical reactions were unable to synthesize HCOOH in the observed abundance and argued therefore that HCOOH most probably is a so-called parent molecule, i.e., one that is directly sublimated from the cometary surface, rather than synthesized in the coma. In their model, HCOOH was partly formed via the reaction scheme (9) followed by Equation (1). No other channel than the one leading to HCOOH + H in the DR of $HCOOH_2^+$ was included. If the experimental results presented in this paper had been used, HCOOH would have been produced in even lower amounts via gas-phase reactions. As such our findings strengthen the interpretation that formic acid is present in the nuclear ice of comet Hale–Bopp.

5. CONCLUSIONS

The DR of $DCOOD_2^+$ has been investigated at CRYRING. At $\sim$2 meV relative kinetic energy maximally 13% of the DR events lead to only hydrogen losses whereas 87% of the reactions involve rupture of a bond between heavy atoms. The reaction has a thermal rate coefficient of $k(T) = 8.43 \times 10^{-7}$ $(T/300)^{-0.78}$ cm^3 s^{-1}. Incorporating the experimental findings into the UMIST code for astrochemistry improves the agreement between calculated and observed (upper limit) abundance of HCOOH in the dark cloud TMC-1. The results also make the interpretation of HCOOH as a parent molecule in comet Hale–Bopp even stronger.

We thank the staff at the Manne Siegbahn Laboratory for excellent technical support. W.D.G. thanks the Swedish Research Council for his Senior Researcher grant (contract No. 2006–427) and the Swedish Space Board (grant No. 76/06). M.K. thanks the Swedish Institute for financial support and also acknowledges support from the Ministry of Science and Higher Education, Poland, under contract N202 111 31/1194. Astrophysics at the Queens University of Belfast is supported by a grant from the STFC. C.W. thanks DEL for a studentship.

REFERENCES

Bockelée-Morvan, D., et al. 2000, A&A, 353, 1101
Crapsi, A., Caselli, P., Walmsley, C. M., Myers, P. C., Tafalla, M., Lee, C. W., & Bourke, T. L. 2005, ApJ, 619, 379
Danared, H., et al. 2000, Nucl. Instr. Meth. A, 441, 123
Datz, S., Sundström, G., Biedermann, C., Broström, L., Danared, H., Mannervik, S., Mowat, J. R., & Larsson, M. 1995, Phys. Rev. Lett., 74, 896
DeWitt, D. R., Schuch, R., Gao, H., Zong, W., Asp, S., & Biedermann, C. 1996, Phys. Rev. A, 53, 2327
Dickens, J. E., Irvine, W. M., Snell, R. L., Bergin, E. A., Schloerb, F. P., Pratap, P., & Miralles, M. P. 2000, ApJ, 542, 870
Garrod, R. T., & Herbst, E. 2006, A&A, 457, 927
Geppert, W. D., et al. 2006, Faraday Discuss., 133, 177
Hamberg, M., et al. 2007, Mol. Phys., 105, 899
Hellberg, F., et al. 2005, J. Chem. Phys., 122, 224314
Herbst, E. 1985, ApJ, 291, 226
Irvine, W. M., Friberg, P., Kaifu, N., Matthews, H. E., Minh, Y. C., Ohishi, M., & Ishikawa, S. 1990, A&A, 229, L9
Lampert, A., Wolf, A., Habs, D., Kettner, J., Kilgus, G., Schwalm, D., Pindzola, M. S., & Badnell, N. R. 1996, Phys. Rev. A, 53, 1413
Leach, S., Schwell, M., Jochims, H.-W., & Baumgärtel, H. 2006, Chem. Phys., 321, 171
Lias, S. G., Bartmess, J. E., Liebman, J. F., Holmes, J. L., Levin, R. D., & Mallard, W. G. 1988, J. Phys. Chem. Ref. Data, Gas-Phase Ion Neutral Thermochem., 17, 1
Liu, S.-Y., Mehringer, D. M., & Snyder, L. E. 2001, ApJ, 552, 654
Matus, M. H., Nguyen, M. T., & Dixon, D. A. 2006, J. Chem. Phys. A, 110, 8864
McCall, B. J., et al. 2004, Phys. Rev. A, 70, 052716
Mowat, J. R., Danared, H., Sundström, G., Carlsson, M., Andersen, L. H., Vejby-Christensen, L., af Ugglas, M., & Larsson, M. 1995, Phys. Rev. Lett., 74, 50
Neau, A., et al. 2000, J. Chem. Phys., 113, 1762
NIST Chemistry Webbook 2005, NIST Standard Reference Database, 69
Ohishi, M., Irvine, W. M., & Kaifu, N. 1992, in IAU Symp. 150, Astrochemistry of Cosmic Phenomena, ed. P. D. Singh (Dordrecht: Kluwer), 171
Paál, A, Simonsson, A., Dietrich, J., & Mohos, I. 2006, in Proc. EPAC 2006, European Particle Conference Particle Accelerator Conference (Edinburgh: European Physical Society Accelerator Group), 1196
Pagani, L., Pardo, J.-R., Apponi, A., Bacmann, A., & Cabrit, S. 2005, A&A, 429, 181
Pagani, L., et al. 2003, A&A, 406, L59
Peterson, J. R., et al. 1998, J. Chem. Phys., 108, 1978
Pratap, P., Dickens, J. E., Snell, R. L., Miralles, M. P., Bergin, E. A., Irvine, W. M., & Schloerb, F. P. 1997, ApJ, 486, 862
Roberts, H., & Herbst, E. 2002, A&A, 395, 233
Roberts, H., & Millar, T. J. 2000, A&A, 364, 780
Rodgers, S. D., & Charnley, S. B. 2001, MNRAS, 320, L61
Rowe, B. R., Dupeyrat, G., Marquette, J. B., Smith, D., Adams, N. G., & Ferguson, E. E. 1984, J. Chem. Phys., 80, 241
Roueff, E., Tiné, S., Coudert, L. H., Pineau des Forêts, G., Falgarone, E., & Gerin, M. 2000, A&A, 354, L63
Sekigushi, O., Bakken, V., & Uggerud, E. 2004, J. Am. Soc. Mass Spectrom., 15, 982
Smith, I. W. M., Herbst, E., & Chang, Q. 2004, MNRAS, 350, 323
Strömholm, C., Semaniak, J., Rosén, S., Danared, H., Datz, S., van der Zande, W., & Larsson, M. 1996, Phys. Rev. A, 54, 3086
Strasser, D., et al. 2002, Phys. Rev. A, 66, 032719
Sundström, G., et al. 1994, Science, 263, 785
Terzieva, R., & Herbst, E. 1998, ApJ, 501, 207
Van Doren, J. M., Barlow, S. E., DePuy, C. H., Bierbaum, V. M., Dotan, I., & Ferguson, E. E. 1986, J. Phys. Chem., 90, 2772
Ward-Thompson, D., Motte, F., & Andre, P. 1999, MNRAS, 305, 143
Winnewisser, G., & Churchwell, E. 1975, ApJ, 200, L33
Woodall, J., Agúndez, M., Markwick-Kemper, A. J., & Millar, T. J. 2007, A&A, 466, 1197
Zuckerman, B., Ball, J. A., & Gottlieb, C. A. 1971, ApJ, 163, L41